



HAL
open science

8-Bromo-cyclic inosine diphosphoribose: towards a selective cyclic ADP-ribose agonist

Tanja Kirchberger, Christelle Moreau, Gerd K. Wagner, Ralf Fliegert, Cornelia C. Siebrands, Merle Nebel, Frederike Schmid, Angelika Harneit, Francesca Odoardi, Alexander Flügel, et al.

► **To cite this version:**

Tanja Kirchberger, Christelle Moreau, Gerd K. Wagner, Ralf Fliegert, Cornelia C. Siebrands, et al.. 8-Bromo-cyclic inosine diphosphoribose: towards a selective cyclic ADP-ribose agonist. *Biochemical Journal*, 2009, 422 (1), pp.139-149. 10.1042/BJ20082308 . hal-00479133

HAL Id: hal-00479133

<https://hal.science/hal-00479133>

Submitted on 30 Apr 2010

HAL is a multi-disciplinary open access archive for the deposit and dissemination of scientific research documents, whether they are published or not. The documents may come from teaching and research institutions in France or abroad, or from public or private research centers.

L'archive ouverte pluridisciplinaire **HAL**, est destinée au dépôt et à la diffusion de documents scientifiques de niveau recherche, publiés ou non, émanant des établissements d'enseignement et de recherche français ou étrangers, des laboratoires publics ou privés.

8-Bromo-cyclic inosine diphosphoribose: towards a selective cyclic ADP-ribose agonist

Tanja KIRCHBERGER^{*}, Christelle MOREAU[†], Gerd K. WAGNER^{†,‡}, Ralf FLIEGERT^{*}, Cornelia C. SIEBRANDS^{*}, Merle NEBEL^{*}, Frederike SCHMID^{*}, Angelika HARNEIT^{*}, Francesca ODOARDI[§], Alexander FLÜGEL[§], Barry V. L. POTTER[†], and Andreas H. GUSE^{*,□}

^{*}The Calcium Signalling Group, University Medical Center Hamburg-Eppendorf, Center of Experimental Medicine, Institute of Biochemistry and Molecular Biology I: Cellular Signal Transduction, Martinistrasse 52, D-20246 Hamburg, Germany

[†]Wolfson Laboratory of Medicinal Chemistry, Department of Pharmacy and Pharmacology, University of Bath, Claverton Down, Bath, BA2 7AY, United Kingdom

[§]Department of Neuroimmunology, Institute for Multiple-Sclerosis-Research, University of Göttingen, Waldweg 33, 37073 Göttingen, Germany

[□]To whom correspondence should be addressed. Phone: ++49-40-7410-52828. Fax: ++49-40-7410-59880. E-mail: guse@uke.uni-hamburg.de

Short title: Ca²⁺ mobilization by the cADPR analogue 8-Br-N1-clDPR

Abbreviations: $[Ca^{2+}]_i$, free cytosolic Ca^{2+} concentration; cADPR, cyclic adenosine 5'-diphosphoribose; ADPRC, ADP-ribosyl cyclase; TBAHP, tetrabutylammonium dihydrogen phosphate; 8-Br-N1-cIDPR, 8-bromo-cyclic inosine 5'-diphosphoribose; 8-Br-IDPR, 8-bromo inosine 5'-diphosphoribose; 8-Br-cADPR, 8-bromo-cyclic adenosine 5'-diphosphoribose; NFAT, nuclear factor of activated T cells; RT, room temperature; RP-HPLC, reversed phase high-performance liquid chromatography; NCS, newborn calf serum; TCA, trichloroacetic acid; TFA, trifluoroacetic acid.

Footnotes:

† Current address: School of Chemical Sciences and Pharmacy, University of East Anglia, Norwich, NR4 7TJ, UK

Synopsis.

Cyclic ADP-ribose (cADPR) is a universal Ca^{2+} mobilizing second messenger. In T cells cADPR is involved in sustained Ca^{2+} release and also in Ca^{2+} entry. Potential mechanisms for the latter include either capacitative Ca^{2+} entry secondary to store depletion by cADPR or direct activation of the non-selective cation channel transient receptor potential – melastatin type 2 (TRPM2). Here we characterize the molecular target of the newly-described membrane-permeant cADPR agonist 8-bromo-cyclic inosine diphosphoribose (8-Br-N1-cIDPR).

8-Br-N1-cIDPR evoked Ca^{2+} signalling in the human T-lymphoma cell line Jurkat and in primary rat T-lymphocytes. Ca^{2+} signalling induced by 8-Br-N1-cIDPR consisted of Ca^{2+} release and Ca^{2+} entry. While Ca^{2+} release was sensitive to both the ryanodine receptor blocker ruthenium red and the cADPR antagonist 8-bromo-cyclic adenosine diphosphoribose (8-Br-cADPR), Ca^{2+} entry was inhibited by the Ca^{2+} entry blockers Gd^{3+} and SKF 96365 as well as by 8-Br-cADPR. To unravel a potential role for TRPM2 in sustained Ca^{2+} entry evoked by 8-Br-N1-cIDPR, TRPM2 was overexpressed in HEK 293 cells. However, though activation by hydrogen peroxide was enhanced dramatically in those cells, Ca^{2+} signalling induced by 8-Br-N1-cIDPR was almost unaffected. Similarly, direct analysis of TRPM2 currents did not reveal activation or co-activation of TRPM2 by 8-Br-N1-cIDPR. In summary, the sensitivity to the Ca^{2+} entry blockers Gd^{3+} and SKF 96365 is in favour of the concept of capacitative Ca^{2+} entry secondary to store depletion by 8-Br-N1-cIDPR. Taken together, 8-Br-N1-cIDPR appears to be the first cADPR agonist affecting Ca^{2+} release (and secondary Ca^{2+} entry), but without effect on TRPM2.

Keywords. cADPR, cADPR analogue, Ca^{2+} release, Ca^{2+} entry, TRPM2, T cell activation.

INTRODUCTION

Cyclic ADP-ribose (cADPR) is a universal Ca^{2+} mobilizing second messenger (reviewed in [1-4]). Receptor-mediated formation has been demonstrated for several cell types and multiple ligands/receptors (reviewed in [1-4]). Formation of cADPR in eukaryotic cells proceeds via ADP-ribosyl cyclase among which the multifunctional ectoenzyme CD38 is best characterized (reviewed in [5]). Originally, cADPR was discovered as endogenous nucleotide to release Ca^{2+} from intracellular stores of sea urchin eggs [6, 7]. However, involvement of cADPR in Ca^{2+} entry was discovered in 1997 in human T-lymphocytes [8].

Ca^{2+} entry in T-lymphocytes is a process essential for proliferation, since a continuously elevated level of the free cytosolic and nuclear Ca^{2+} concentration ($[\text{Ca}^{2+}]_i$) is necessary for continuous activation of Ca^{2+} /calmodulin-dependent protein phosphatase calcineurin [9]. The latter dephosphorylates nuclear factor of activated T cells (NF-AT) thereby allowing translocation of NF-AT into the nucleus [10, 11].

As mechanism for Ca^{2+} entry in T cells, capacitative Ca^{2+} entry [12] has long been postulated (reviewed in [13]). With the discovery of key proteins involved, e.g. Orai1/CRACM1 [14, 15] and Stim 1 [16], it became clear that Stim1, by sensing decreasing luminal Ca^{2+} concentration upon store depletion, would activate Ca^{2+} entry involving Orai1/CRACM1 as channels or as part of a larger channel complex. In T-lymphocytes we have demonstrated a crucial role for cADPR in Ca^{2+} entry, since blockade of cADPR action resulted in reduced Ca^{2+} signalling, especially in the sustained phase [17]. Importantly, subsequent signalling events, e.g. CD25 and MHC-II expression and proliferation were likewise inhibited by cADPR antagonism [17].

Here, we characterize the Ca^{2+} entry mechanism activated by the novel cADPR agonist, 8-Br-N1-cIDPR [18]. The advantages of this molecule over natural cADPR are its ability to permeate membranes and its metabolic stability. Indeed, we recently showed that substitution of the amino/imino-group at C6 by an oxo-group, thus converting the bond between N1 and C1'' at the northern ribose into part of a much more chemically stable, amide system, produces a compound that is also biologically stable.

EXPERIMENTAL

Drugs and materials

8-Br-NHD and cADPR were obtained from Biolog (Bremen, Germany). 8-Br-N1-cIDPR was either synthesized and purified by some of the authors as described below (see also Fig. 1) or, at later stages, obtained from Biolog (Bremen, Germany). ADP-ribosyl cyclase from *Aplysia californica*, 8-Br-cADPR and GdCl₃ were purchased from Sigma-Aldrich (München, Germany). Ruthenium red, SKF96365, trichloroacetic acid (TCA), diethyl ether, methanol (LiChrosolv) and trifluoroacetic acid (TFA) were procured from Calbiochem/Merck (Darmstadt, Germany). Rat CD3 antibody, goat anti-mouse IgM and Lipofectamine 2000 were obtained from Caltag Laboratories/Invitrogen (Carlsbad, USA). Q-Sepharose Fast Flow and G10 Sephadex were obtained from Amersham Bioscience (Freiburg, Germany). FuGENE 6 was procured from Roche Applied Science (Indianapolis, USA). All other chemicals used were of the highest purity grade and purchased from Calbiochem/Merck, Fluka (Buchs, Switzerland) or Sigma-Aldrich. Culture medium reagents were supplied by Sigma-Aldrich, GIBCO-Invitrogen (Auckland, New Zealand) or Biochrom (Berlin, Germany).

Cell culture

Jurkat T-lymphocytes (subclone JMP) were cultured as described previously [19] at 37°C in the presence of 5 % CO₂ in RPMI 1640 medium containing Glutamax I and HEPES (25 mM) and supplemented with 7.5 % (v/v) newborn calf serum (NCS), 100 units/ml penicillin and 100 µg/ml streptomycin.

MBP-specific T cell clones were established from lymph node preparations of pre-immunized Lewis rats. Stimulation, expansion and culture of specific rat T cells were conducted under conditions as described [20]. For determination of Ca²⁺ signalling, frozen rat T cells were thawed and cultured in DMEM with Glutamax I, 4.5 g/l glucose, 100 units/ml penicillin, 100 µg/ml streptomycin, 1 mM sodium pyruvate, 10 % (v/v) horse serum, 0.004 % (v/v) 2-mercaptoethanol, 1 % (v/v) non-essential amino acids, 0.04 g/l asparagine at 37 °C in the presence of 10 % CO₂. Resting state T cells were used in all experiments.

HEK293 cells were cultured at 37°C in the presence of 5 % CO₂ in DMEM medium containing Glutamax I and supplemented with 10 % (v/v) fetal bovine serum (FBS), 100 units/ml penicillin and 100 µg/ml streptomycin.

Synthesis and purification of 8-Br-N1-cIDPR

8-Br-N1-cIDPR was synthesized as previously described [21]. 100 µmol 8-Br-NHD were incubated with 40 µg *A.californica* ADP-ribosyl cyclase in 25 mM HEPES pH7.4 for 15 h at room temperature under continuous stirring in the dark. ADP-ribosyl cyclase was removed by stepwise centrifugation for 1 to 2 h at 4000 g and 4°C by use of centrifugal filter devices type Centriprep YM-10 (10 kDa MW cut-off; Millipore). Synthesis of 8-Br-N1-cIDPR was confirmed by RP-HPLC. Purification was carried out as previously described [21] or by another strategy in two steps by anion exchange chromatography and gelfiltration to remove the byproducts 8-Br-IDPR and nicotinamide. For anion exchange chromatography Q-Sepharose FF was washed 4 times with water, 4 times with 500 mM NaCl and 5 times with purified Milli-Q water (Millipore Waters, Eschborn, Germany). 0.5 ml Q-Sepharose FF were packed in plastic filtration tubes (Supelco, Bellefonte, USA) and washed with 10 ml purified water. The aqueous solution of 8-Br-N1-cIDPR was diluted 5-times with purified water to reduce ionic strength and applied to the column in 3 ml aliquots. The column was washed 2 times with 5 ml purified water. Elution of 8-Br-N1-cIDPR was carried out by subsequent addition of 1.5 ml NaCl solution portions of 20, 40, 60, 80, 100, 120, 140, 160, 180, 200 or 250 mM. The eluates were collected and analyzed by RP-HPLC. Eluates contained only 8-Br-N1-cIDPR (40 to 100 mM NaCl) were combined. Purified 8-Br-N1-cIDPR was desalted by gelfiltration on Sephadex G10. For gelfiltration, 30 g Sephadex G10 was suspended in 100 ml water, heated for 1 h at 90 °C and washed 4 times with water. A suspension with 75 % (w/v) Sephadex G10 was prepared, degassed, packed in a glass column (1.5 x 30 cm) and compacted for 16 h by gravity flow of water. The solution of 8-Br-N1-cIDPR was chromatographed with water as eluent. Eluates were collected in a volume of 1 to 5 ml, analyzed by RP-HPLC, combined and lyophilized. Final characterization of purity and identity was done on RP-HPLC (see Fig. 1).

Determination of membrane permeability of 8-Br-N1-cIDPR

Jurkat T cells (2 to 2.5 x10⁸) were harvested by centrifugation, washed once with buffer A containing 140 mM NaCl, 5 mM KCl, 1 mM MgSO₄, 1 mM CaCl₂, 1 mM NaH₂PO₄, 5.5 mM glucose, 20 mM

HEPES, pH 7.4, resuspended in 1 ml buffer A and kept at room temperature for 10 min. 3 μ mol 8-Br-*N1*-cIDPR were added, cells were incubated for 5 min at RT, placed on an ice-salt bath for 3 min, harvested by centrifugation at 4°C and washed once with 5 ml ice cold buffer A. Determination of 8-Br-*N1*-cIDPR was performed in a similar way as previously described for endogenous ADPR [22]. Briefly, cells were lysed in trichloroacetic acid, and cell debris was removed. The samples were divided into identical halves, to one of which 50 nmol 8-Br-*N1*-cIDPR was added to identify the 8-Br-*N1*-cIDPR peak by HPLC and to calculate the recovery during the extraction. Protein precipitates were removed, and the supernatants were neutralized by extraction with diethyl ether. The samples were then purified by solid phase extraction. For solid phase extraction plastic filtration tubes (Supelco, Bellefonte, USA) were packed with Q-Sepharose FF and were cleaned in place with 150 mM TFA. Columns were equilibrated with 10 mM Tris-HCl, pH 8.0. The cellular extracts were diluted with 10 mM Tris-HCl, pH 8.0 and applied to the columns. The columns were washed first with 10 mM Tris-HCl, pH 8.0 followed by 600 μ l 40 mM TFA. For the elution of 8-Br-*N1*-cIDPR, 1 ml of a 80 mM TFA solution was applied. Samples were neutralized by NaOH, filtered through 0.2 μ m filters (Sartorius, Göttingen, Germany) and analyzed by RP-HPLC as described below. As a control the non-brominated dinucleotide nicotinamide hypoxanthine dinucleotide (NHD) was used in parallel.

Reversed Phase-HPLC

RP-HPLC analysis of nucleotides was performed on a 250x4.6mm Multohyp BDS C18-5 μ column (CS Chromatographie Service, Langerwehe, Germany) equipped with a 17x4.6mm guard column filled with the same column material or with a 4.0x3.0 guard cartridge containing a C18 (ODS) filter element (Phenomenex, Aschaffenburg, Germany). The separation was performed as described previously [23] at a flow rate of 1 ml/min with RP-HPLC buffer (20 mM KH₂PO₄, 5 mM tetrabutylammonium dihydrogen phosphate, pH 6) containing increasing amounts of methanol. The gradient used for separation was usually (% methanol) 0 min (6.5), 3.5 min (7.5), 5.5 min (16), 8 min (25), 18 min (6.5) and 27 min (6.5). For separation of 8-Br-*N1*-cIDPR in cell extracts the following gradient was used (% methanol) 0 min (6.5), 1.5 (6.5), 3.5 min (7.5), 5.5 min (16), 6.5 min (16), 14 min (32.5), 16 min (32.5), 18 min (6.5) and 27 min (6.5). Nucleotides were detected using an UV detector (HPLC detector 432, Kontron Instruments, Neufahrn, Germany) or a DAD (photo diode array detector 1200 series, Agilent technologies) at 250 nm or 260 nm for hypoxanthine or at 270 nm for adenine based nucleotides, respectively. Integration of peaks was performed with the data-acquisition system MT2 from Kontron Instruments or ChemStation from Agilent technologies (Rev. B.02.01). Quantification was performed with external standards.

Transient Transfection of HEK293 cells

A cDNA containing the total ORF of human TRPM2 was amplified from human RNA by one-step RT-PCR using Titan one-Tube RT-PCR system (Roche, Mannheim, Germany) according to the manufacturer's instructions (forward primer including *Eco*RI site: 5'-ggaattcatggagccctcagccctg-3'; reverse primer including a *Sal*I site: 5'-tactgtcgactcagtagtgagccc-3'). The resulting amplicon was cloned into the *Eco*RI and *Sal*I sites of the multiple cloning site of pIRES2-EGFP (Clontech, Heidelberg, Germany). This vector was termed pIRES2-EGFP-TRPM2.

For transfection, HEK293 cells were seeded in 35 mm dishes, cultured to a density of 50 to 80 % of confluency and were transfected by addition of transfection mixture consisting of 100 μ l OptiMEM, 3 μ l FuGENE or 3 μ l Lipofectamine 2000 and 1 μ g plasmid DNA (pIRES2-EGFP or pIRES2-EGFP-TRPM2) to the cells. For transfection with FuGENE transfection mixture was added directly to the cell culture medium, whereas transfection with Lipofectamine 2000 was carried out in OptiMEM. For Ca²⁺-imaging experiments, transfected cells were seeded in 8-well slides (ibidi, Martinsried, Germany) coated with poly-L-lysine (70-150 kDa) at low cell density.

Ratiometric Ca²⁺ imaging

Jurkat T cells were loaded with Fura-2/AM as described [19] and kept in the dark at room temperature until use. Primary rat T cells were loaded with 12 μ M Fura2/AM and 2 mM probenidol for 30 min at 37°C in the dark and washed twice with buffer A and kept in the dark at 15 – 18 °C until use. HEK293 cells were loaded in 8-well slides with 4 μ M Fura 2/AM in HEK293 cell media for 30 min at 37°C in the dark and washed twice with buffer A.

For Ca²⁺ imaging of Jurkat T cells or rat T cells thin glass coverslips (0.1 mm) were coated first with BSA (5 mg/ml) and subsequently with poly-L-lysine (0.06 - 0.1 mg/ml). Silicon grease was used to seal

small chamber slides consisting of a rubber O-ring on the glass coverslip. Then, 40 - 60 μl buffer A and 40 μl T cell suspension ($1 - 2 \times 10^6$ cells/ml) suspended in the same buffer were added into the small chamber. Where the calcium free/calcium re-addition protocol was used, 0.2×10^6 Jurkat T cells were washed twice in nominal Ca^{2+} -free buffer A and added to the small chamber. The time span the cells were held under Ca^{2+} free conditions was kept as short as possible to avoid emptying of the ER Ca^{2+} pool; such emptying due to prolonged exposure to Ca^{2+} free conditions resulted in very low or undetectable Ca^{2+} signals upon cADPR microinjections in a previous study [8]. The loaded coverslip or 8-well slide was mounted on the stage of a fluorescence microscope (Leica DMIRE2). In some experiments Jurkat T cells were preincubated with GdCl_3 (25 μM), SKF 96365 (30 μM) or 8-Br-cADPR (500 μM) in buffer A. In experiments with GdCl_3 Na_2HPO_4 was not included in buffer A to prevent precipitation of GdPO_4 .

Ratiometric Ca^{2+} imaging was performed as described recently [24]. We used an Improvion imaging system (Tübingen, Germany) built around the Leica microscope at 40- or 100-fold magnification. Illumination at 340 and 380 nm was carried out using a monochromator system (Polychrom IV, TILL Photonics, Gräfelfing, Germany). Images were taken with a gray-scale CCD-camera (type C 4742-95-12ER; Hamamatsu, Enfield, United Kingdom) operated in 8-bit mode. The spatial resolution was 512 x 640 pixels. Camera exposure times were 12 - 30 ms (at 340 nm) and 4 - 10 ms (at 380 nm) at a 3:1 ratio. The acquisition rate was adjusted to ~14 ratios per minute. Raw data images were stored on a hard disk and ratio images (340/380 nm) were constructed pixel by pixel. Confocal Ca^{2+} images were obtained by off-line deconvolution (no-neighbor algorithm) using the volume deconvolution module of the Openlab software as described recently for 3T3 fibroblasts [25]. The deconvoluted images were used to construct ratio images (340/380 nm) pixel by pixel. Finally, ratio values were converted into Ca^{2+} concentrations by external calibration [24]. Data processing was performed using Openlab software, version 3.0.8 or 1.7.8 (Improvion, Tübingen, Germany).

Microinjection

Microinjections were carried out as described [8]. We used an Eppendorf system (transjector type 5171, micromanipulator type 5246 or Femtojet (Eppendorf AG, Hamburg, Germany) with Femtotips I or II as pipettes. 8-Br-N1-cIDPR or cADPR were diluted to their final concentration in intracellular buffer (20 mM HEPES, 110 mM KCl, 10 mM NaCl, pH 7.2), filtered (0.2 μm) and centrifuged (15700 g, 10 min, 4°C) before use. Injections were made using the semiautomatic mode of the system with following instrumental settings: injection pressure 60 to 80 hPa, compensatory pressure 25 to 40 hPa, injection time 0.5 sec and velocity of the pipette 700 $\mu\text{m}/\text{sec}$.

Electrophysiology

Membrane currents were recorded in the whole cell configuration of the patch clamp technique [26]. An EPC10 USB patch clamp amplifier was used in conjunction with the PULSE stimulation and data acquisition software (HEKA Elektronik, Lamprecht, Germany). Data were sampled at 5 kHz and compensated for both fast and slow capacity transients. Series resistance was compensated by 70%. All experiments were performed at room temperature with Jurkat T cells attached to tissue culture dishes before the experiment. The pipette solution contained 140 mM KCl, 1 mM MgCl_2 , 8 mM NaCl and 10 mM HEPES adjusted to pH 7.2 with KOH. In some experiments, the pipette solution additionally contained ADPR (30, 100, 300 or 1000 μM), cADPR (30, 100, 300 or 1000 μM), 8-Br-N1-cIDPR (300 μM), ADPR (30 μM) plus either cADPR (5 μM or 100 μM) or 8-Br-N1-cIDPR (300 μM). The external solution contained 140 mM NaCl, 2 mM MgCl_2 , 2 mM CaCl_2 , 5 mM KCl, 10 mM HEPES, and 5 mM glucose adjusted to pH 7.4 with NaOH. The cells were held at -60 mV and current-voltage relations were obtained every 5 s using 250-ms voltage ramps from -85 to -65 mV.

RESULTS

8-Br-N1-cIDPR was prepared by quantitative conversion of 8-Br-NHD to 8-Br-N1-cIDPR using *Aplysia californica* ADP-ribosyl cyclase (Fig. 1). Comparison of the products after a 15 h incubation period with standards clearly showed that the main product was 8-Br-N1-cIDPR. However, a small portion of 8-Br-NHD was converted to the linear product 8-Br-IDPR (Fig. 1d). This small contamination of 8-Br-IDPR was quantitatively removed by anion exchange chromatography using Sepharose Q fast flow followed by desalting of purified 8-Br-N1-cIDPR on Sephadex 10 fast flow. The final product showed a purity of almost 100% on HPLC (Fig. 1e).

Though we had reported earlier in a preliminary communication that 8-Br-N1-cIDPR is membrane-permeant, initially the biological activity of 8-Br-N1-cIDPR was assessed in combined microinjection and Ca^{2+} imaging experiments to obtain a proper concentration-response relationship without any potential additional effects due to membrane permeancy and/or pumping out of the compound by multiple drug resistance transporters. While microinjection of intracellular buffer into intact Fura2-loaded Jurkat T cells had little effect (Fig. 2 a), the natural cADPR showed a robust response when microinjected at 100 μM (Fig. 2 b). It must be noted here that in such microinjection experiments only about 1 to 1.5 % of the cell volume is injected [8] resulting in an effective intracellular concentration far below the pipette concentration. At 100 μM 8-Br-N1-cIDPR evoked Ca^{2+} signalling only in some cells (Fig. 2 c), whereas at pipette concentrations ≥ 1 mM of 8-Br-N1-cIDPR, robust Ca^{2+} responses were recorded consisting of a rapid and high Ca^{2+} peak within tens of seconds followed by a lower, but sustained plateau phase (Fig. 2 d to f). The effect was saturable and showed an EC_{50} of about 300 μM (Fig. 2g).

Importantly, the 8-substitution with bromine in 8-Br-N1-cIDPR resulted in a membrane-permeant molecule, as already determined in initial experiments [21]. To check the membrane permeability of 8-Br-N1-cIDPR directly, Jurkat T cells were incubated with 8-Br-N1-cIDPR for 5 min; then, cellular nucleotides were extracted with trichloroacetic acid; and crude cell extracts were purified by solid phase extraction and analysed by RP-HPLC (Fig. 3 a, b) in a similar way as described for ADPR [22]. In Jurkat T cells incubated with 8-Br-N1-cIDPR a cellular uptake of 0.16 fmol/cell was measured (Fig. 3). In contrast, cells incubated with the non-brominated dinucleotide NHD did not take up this molecule indicating that bromination is a prerequisite for membrane permeancy (data not shown). In separate experiments, we checked that NHD was not metabolized in the time period of the uptake experiments.

Addition of membrane permeant 8-Br-N1-cIDPR to intact Jurkat T cells induced a dose dependent Ca^{2+} signal (Fig. 4). At concentrations ≥ 1 mM 8-Br-N1-cIDPR a rapid Ca^{2+} response in these cells consisting of a Ca^{2+} peak and a small but sustained plateau phase was observed (Fig. 4c), whereas no Ca^{2+} signal was mediated by addition of the non brominated analogue N1-cIDPR (Fig. 4b) or buffer (Fig. 4a). Since 8-Br-N1-cIDPR at 1 mM induced robust and significant Ca^{2+} signalling, this extracellular concentration was chosen for most further experiments.

To test the effect of 8-Br-N1-cIDPR also on primary T cells, rat myelin-basic protein (MBP)-specific T cells were loaded with Fura2/AM and subjected to Ca^{2+} imaging (Fig. 5). Buffer was added as a negative control, while cells were stimulated via the T cell receptor/CD3 complex (anti CD3/IgM) as a positive control (Fig. 5 a, b). Though anti-CD3 antibody alone resulted in a robust Ca^{2+} signal, crosslinking of the primary antibody on the surface of the cells further enhanced the stimulation (Fig. 5 b). Addition of 8-Br-N1-cIDPR resulted in Ca^{2+} signals with different kinetics and amplitudes with regard to individual cells (Fig. 5 c). When compared to T cell receptor/CD3 stimulation, similar individual differences in kinetics were observed (compare Fig. 5b and c), whereas peak amplitudes were significantly lower for 8-Br-N1-cIDPR (Fig. 5d). This difference is not unexpected since in the first 10 minutes of T cell activation, at least three Ca^{2+} release systems (nicotinic acid adenine dinucleotide phosphate (NAADP), D-myoinositol 1,4,5-trisphosphate (IP_3) and cADPR; (reviewed in [3, 27]) are involved. However, 8-Br-N1-cIDPR mimicked the second phase of TCR/CD3 mediated Ca^{2+} signalling once again underpinning the essential role of cADPR in sustained Ca^{2+} signalling in T cells.

cADPR has been shown to act both on intracellular Ca^{2+} release via RyR [17], but also to sensitize TRPM2 cation channel for its ligand ADPR [28, 29]. To analyze the mechanism of the cADPR analogue 8-Br-N1-cIDPR in more detail, a Ca^{2+} free/ Ca^{2+} reintroduction protocol was used to separate potential Ca^{2+} release and Ca^{2+} entry evoked by 8-Br-N1-cIDPR (Fig. 6). Under Ca^{2+} free conditions, a robust Ca^{2+} release upon addition of 8-Br-N1-cIDPR was observed (Fig. 6 a,b). Re-addition of extracellular Ca^{2+} resulted in a huge Ca^{2+} entry overshoot followed by a small sustained plateau phase (Fig. 6 a, b). These data suggest that 8-Br-N1-cIDPR activates both Ca^{2+} release and Ca^{2+} entry.

Secondly, co-microinjections of 8-Br-N1-cIDPR with ruthenium red (RuRed) were carried out (Fig. 7). RuRed largely reduced the initial Ca^{2+} peak (Fig. 7 c,d) indicating that this initial peak mainly depends on RyR.

Taken together, we showed that 8-Br-N1-cIDPR behaved similarly to what we currently know about cADPR. In the next sets of experiments we aimed to analyze in more detail the Ca^{2+} entry pathway activated by 8-Br-N1-cIDPR. Thus, we used inhibitors of Ca^{2+} entry, e.g. GdCl_3 and SKF 96365 [8, 30, 31]. In both cases robust Ca^{2+} release was observed under Ca^{2+} free conditions, while Ca^{2+} entry was inhibited (Fig. 8 c,d,g,h). Interestingly, preincubation with Gd^{3+} increased Ca^{2+} release induced by 8-Br-N1-cIDPR significantly (Fig. 8 d). A potential explanation for this effect is the sensitivity of the plasma

membrane Ca^{2+} ATPase towards Gd^{3+} [32]; inhibition of Ca^{2+} extrusion in the absence of extracellular Ca^{2+} would in fact result in an apparent increase of $[\text{Ca}^{2+}]_i$.

In the presence of the cADPR antagonist 8-Br-cADPR, Ca^{2+} release was partially, but not significantly inhibited (Fig. 8 k,l). Interestingly, there was full inhibition of Ca^{2+} entry under such conditions. Likely, the incomplete inhibition of Ca^{2+} release is due to the partial antagonist character of 8-Br-cADPR [33]. As discussed above for Ca^{2+} entry, at least two mechanisms may be involved: either the diminished Ca^{2+} release resulted in inhibition of capacitative Ca^{2+} entry via Orai1/CRACM1 channels [34] or direct activation of Ca^{2+} entry by 8-Br-N1-cIDPR was inhibited by 8-Br-cADPR. Since Kolisek et al. [28] recently showed that cADPR together with ADPR activates the unspecific cation channel TRPM2, we used HEK 293 cells transiently overexpressing TRPM2 or EGFP (as negative control) for further experiments. As positive control, Ca^{2+} signalling induced by hydrogen peroxide was used since it was recently shown that hydrogen peroxide increased the open probability of TRPM2 [28, 35]. These results were confirmed (Fig. 9 a,d). In contrast, statistically significant effects between TRPM2 overexpressing cells or controls were not obtained when 8-Br-N1-cIDPR was used as activator of Ca^{2+} signalling up to extracellular concentrations of 10 mM (Fig. 9 b, e, g).

In the next series of experiments direct activation of endogenously expressed TRPM2 in Jurkat T cells was analyzed by patch-clamp recordings in the whole-cell configuration. Infusion of ADPR (300 μM) at a membrane potential of -80 mV evoked a marked inward current (Fig. 10 a) characterized by an almost linear IV-relationship (Fig. 10 b) and a saturable concentration-response relationship with an EC_{50} of 133 μM (Fig. 10 c). Infusion of cADPR alone did not activate the TRPM2 current except showing a minor effect at 1 mM cADPR pipette concentration (Fig. 10 c). However, due to the small contamination of 4% ADPR (Fig. 10 e) amounting to 40 μM ADPR (!) in the pipette, it is likely that this ADPR contamination, and not the cADPR in the pipette, induced the current. Comparing the amplitudes evoked by 30 μM ADPR and 1 mM cADPR (containing 40 μM ADPR) further substantiates this conclusion (Fig. 10 c). Infusion of combination of a low concentration of ADPR (30 μM) plus cADPR had a small modulatory effect when 100 μM cADPR was used (Fig. 10 d) indicating a co-modulatory role of cADPR on TRPM2 activated by low concentrations of ADPR as described [35]. However, 8-Br-N1-cIDPR neither activated TRPM2 alone (Fig. 10 c) nor in combination with low ADPR (Fig. 10 d).

DISCUSSION

In this report we demonstrate that the membrane-permeant cADPR agonist 8-Br-N1-cIDPR evokes Ca^{2+} signalling in both the T-lymphoma cell line Jurkat and in primary T cells. Ca^{2+} signalling induced by 8-Br-N1-cIDPR consisted of both Ca^{2+} release and Ca^{2+} entry. While Ca^{2+} release was sensitive to both the RyR blocker ruthenium red and the cADPR antagonist 8-Br-cADPR, Ca^{2+} entry was inhibited by the non-specific Ca^{2+} entry blockers Gd^{3+} and SKF 96365 as well as by 8-Br-cADPR [10]. Activation of TRPM2 by 8-Br-N1-cIDPR was neither observed in heterologously expressed TRPM2 in HEK cells activated by H_2O_2 nor in endogenously expressed TRPM2 in Jurkat T cells. Further, 8-Br-N1-cIDPR did not co-activate TRPM2 when infused together with a low concentration of ADPR.

Stimulation of T cell Ca^{2+} signalling via the T cell receptor/CD3 complex involves the subsequent formation of at least three second messengers. Within a few seconds NAADP is produced peaking around 10 to 20 seconds and returning to the baseline rapidly [36]. NAADP serves as initial Ca^{2+} trigger to "ignite" the Ca^{2+} signalling system of T cells (for review see [37]). Next, IP_3 is produced transiently and initiates global Ca^{2+} signalling within the first 15 to 20 min of T cell activation [38]. In contrast, cADPR is formed more slowly and continues to release Ca^{2+} from internal stores as IP_3 levels fall [17]. Thus, sustained elevated cADPR levels and sustained Ca^{2+} signalling by cADPR are essential components of T cell activation [17]. Since the intracellular Ca^{2+} stores of T cells are low in capacity, sustained Ca^{2+} signalling is only possible by recruitment of Ca^{2+} entry. In theory, at least two mechanisms for Ca^{2+} entry evoked by the sustained high cADPR levels are possible: either capacitative Ca^{2+} entry [12] via Orai1/CRACM1 channels [14, 15] is activated by reduced store loading secondary to cADPR action, or cADPR acts as a co-activator of TRPM2 as described recently [28, 29].

As described for a number of membrane-permeant cADPR agonists recently, e.g. N1-ethoxymethyl-cIDPR [39], N1-[(phosphoryl-O-ethoxy)-methyl]-N9-[(phosphoryl-O-ethoxy)-methyl]-hypoxanthine-cyclic pyrophosphate [40], 2",3"-dideoxy-didehydro-cyclic ADP-carbocyclic ribose (2",3"-dideoxy-didehydro-

cADPR) [41], 8-phenyl-cIDPR [42], *N*1-[(5'-*O*-phosphoryl)ethoxyethyl]-5-*O*-phosphoryladenosine 5',5'-cyclic pyrophosphate [43], 8-Br-*N*1-cIDPR essentially mimicks the cADPR branch of T cell Ca²⁺ signalling. However, for none of these cADPR analogues with agonist properties has the mechanism of Ca²⁺ entry been elucidated. Since 8-bromo-nicotinamide hypoxanthine dinucleotide, the synthetic precursor of 8-Br-*N*1-cIDPR, can be easily synthesized in larger quantities and since 8-Br-*N*1-cIDPR can then be formed in high yield chemo-enzymatically [21], we performed this detailed analysis of cADPR-mediated Ca²⁺ entry using 8-Br-*N*1-cIDPR as cADPR agonist. The advantage of this strategy clearly is the precise activation of only the cADPR/RyR branch; the disadvantage is that any signalling crosstalk from other pathways triggered upon T cell activation that may modulate the cADPR/RyR branch is not involved here.

TRPM2 channel opening was described to be regulated by ADPR with a crucial role of cADPR as co-activator [28, 29]. Further, co-activatory effects of cADPR towards TRPM2 are sensitive to the cADPR antagonist 8-Br-cADPR [35]. Since we observed that 8-Br-cADPR effectively inhibits Ca²⁺ entry evoked by 8-Br-*N*1-cIDPR (Fig. 8 k,l), a contribution of TRPM2 appeared possible. To analyze this in more detail, TRPM2 overexpressing HEK 293 cells were challenged with 8-Br-*N*1-cIDPR; however, no significant differences to control cells were observed, though hydrogen peroxide as positive control evoked huge and robust TRPM2 activation. Moreover, also the direct analysis of TRPM2 currents in patch clamp experiments did not reveal any evidence for activation of TRPM2 by 8-Br-*N*1-cIDPR. However, the previously published activation of TRPM2 by cADPR [28, 35] appears to be due to ADPR contamination. This is present in almost all commercially available cADPR preparations. These preparations may contain up to 20% of ADPR (!). The preparation used in our experiments was further purified to a purity of 96%; however, higher purities are very difficult to achieve due to the instability of cADPR in solution and during freeze/thaw cycles. In contrast, a small effect attributable to cADPR was observed when it was co-infused with a low concentration of ADPR. Replacement of cADPR by 8-Br-*N*1-cIDPR in such co-infusion experiments did not evoke TRPM2 currents suggesting that the co-activating effect of cADPR on TRPM2 cannot be mimicked by 8-Br-*N*1-cIDPR.

Activation of Orai1/CRACM1 channels - though not discovered at that time and thus termed capacitative Ca²⁺ entry channels - by cADPR via RyR mediated store depletion was described for DT 40 B lymphoma cells lacking expression of all 3 subtypes of IP₃ receptors [34]. Since we did not find evidence for involvement of TRPM2, activation of capacitative Ca²⁺ entry secondary to cADPR- or 8-Br-*N*1-cIDPR-mediated store depletion appears the most likely process involved. This conclusion is further supported by knock down of type 3 RyR in T cells resulting in significantly diminished sustained Ca²⁺ signalling [44]. Further, the sensitivity of 8-Br-*N*1-cIDPR mediated Ca²⁺ entry to SKF96365 also is in accordance with activation of capacitative Ca²⁺ entry by 8-Br-*N*1-cIDPR. Interestingly, complete inhibition of Ca²⁺ entry was observed upon 8-Br-cADPR preincubation while Ca²⁺ release was only partially inhibited. This obvious contradiction may be explained by the non-linear activation of capacitative Ca²⁺ entry by increasing store depletion [45]. Though this effect was explained partially by metabolism of IP₃ [45], it is not unlikely that also the extent of store depletion is not linearly coupled to activation of capacitative Ca²⁺ entry.

Taken together, we provide a detailed analysis of mode of action of the synthetically easily accessible and membrane-permeant cADPR agonist 8-Br-*N*1-cIDPR. Since 8-Br-*N*1-cIDPR did not activate TRPM2, this cADPR analogue appears to be the first agonist with selectivity towards the targets RyR and TRPM2.

Acknowledgements. We are grateful to the Deutsche Forschungsgemeinschaft for Grants GU 360/9-1 and 9-2 (to AHG.), the Gemeinnützige Hertie-Stiftung, (grant no. 1.01.1/07/005 to AHG and AF), and the Wellcome Trust for Project Grants 55709 (to BVLP) and 084068 (to BVLP and AHG), VIP support and a Biomedical Research Collaboration Grant 068065 (to BVLP and AHG).

Legends of figures

Figure 1 Synthesis of 8-Br-N1-cIDPR

(a) RP-HPLC of standard 1: 8Br-NHD, 8-Br-N1-cIDPR (for reasons of clarity 8-Br-N1-cIDPR is abbreviated as 8Br-cIDPR in all figures). (b) RP-HPLC of standard 2: nicotinamide (NicAmid), 8Br-NHD and 8Br-IDPR; 8Br-IDPR was synthesized by incubation of 8Br-NHD with NADase of *N. crassa*. (c, d) 1 mM 8Br-NHD was incubated with 1 $\mu\text{g}/\mu\text{l}$ ADP-ribosyl cyclase of *A. californica* in 25 mM HEPES pH 7.4 for 15 h at RT. Aliquots were taken at 0 and 15 h and analyzed by RP-HPLC. (e) RP-HPLC of purified 8-Br-N1-cIDPR.

Figure 2 Microinjection of 8-Br-N1-cIDPR in intact Jurkat T cells

Jurkat T cells were loaded with Fura-2 and subjected to combined Ca^{2+} imaging and microinjection. Time points of microinjection are indicated by arrows. Cells were microinjected with intracellular buffer (a; n=21) or 100 μM cADPR (b; n=20) as control and with 0.1 (c; n=6), 1 (d; n=7), 10 (e; n=10) or 100 mM (f; n=5) 8-Br-N1-cIDPR. Concentration-response curve of 8-Br-N1-cIDPR is shown in g. Data are mean \pm S.E. (n= 5- 21) of single tracings from time points 50 – 100 s (Ca^{2+} peak); * p < 0.01, ** p < 0.001 (t-test).

Figure 3 Membrane permeability of 8-Br-N1-cIDPR

Jurkat T cells were incubated with 3 mM 8-Br-N1-cIDPR for 5 min at RT. Cellular nucleotides were extracted with trichloroacetic acid. Crude cell extracts were purified by solid phase extraction and analysed by RP-HPLC. Representative RP-HPLC analysis of absorbed 8-Br-N1-cIDPR in Jurkat T cells is shown (a, b black line). The peak of 8-Br-N1-cIDPR is indicated by an arrow. For control, cell extracts of cells not incubated with 8-Br-N1-cIDPR were analysed by HPLC (a, b grey line). Jurkat T cells incubated with 8-Br-N1-cIDPR took up 0.16 fmol/cell with a recovery of about 88%. Data are mean (n=2).

Figure 4 Extracellular addition of 8-Br-N1-cIDPR evoked Ca^{2+} signalling in intact Jurkat T cells

Jurkat T cells were loaded with Fura-2 and subjected to Ca^{2+} imaging. The time points of addition of buffer (a), 1 mM N1-cIDPR (b) and 1 mM 8-Br-N1-cIDPR (c) are indicated by arrows. Characteristic tracings from a representative experiment are shown (a-c). Concentration-response curve of 8-Br-N1-cIDPR is shown in (d). Data represent mean \pm S.E. (n= 21- 109) of single tracings from time points 100 to 400 s (8-Br-N1-cIDPR mediated Ca^{2+} peak).

Figure 5 Extracellular addition of 8-Br-N1-cIDPR evoked Ca^{2+} signalling in primary rat T cells

Rat T cells were loaded with Fura-2 and subjected to Ca^{2+} imaging. The time points of addition of buffer (a), anti-CD3 followed by a crosslinking IgM (40 $\mu\text{g}/\text{ml}$ and 10 $\mu\text{g}/\text{ml}$; b) and 1 mM 8-Br-N1-cIDPR (c) are indicated by arrows. Characteristic tracings from a representative experiment are shown (a-c). Combined data are shown in d; these represent mean \pm S.E. (n= 186- 241) of single tracings from time points 100 – 400 s (Ca^{2+} peak). * p < 0.01, ** p < 0.001 (t-test).

Figure 6 8-Br-N1-cIDPR activated both Ca²⁺ release and Ca²⁺ entry in intact Jurkat T cells

(a, b) Jurkat T cells were loaded with Fura-2 and subjected to Ca²⁺ imaging. (a) Cells were kept in a nominally Ca²⁺ free buffer in the first part of experiment and 8-Br-N1-cIDPR was added as indicated. Then, CaCl₂ was re-added. (b) Buffer was added instead of 8-Br-N1-cIDPR as control. The time points of addition of buffer, 1 mM 8-Br-N1-cIDPR or 1 mM Ca²⁺ are indicated by arrows. Characteristic tracings from a representative experiment are shown (a, b). Combined data are shown in (c); these represent mean ± S.E. (n= 362 to 404) of single tracings from time points 100 to 200 s (8-Br-N1-cIDPR mediated Ca²⁺ release-peak) or 300 to 450 s (8-Br-N1-cIDPR mediated Ca²⁺ entry-peak). ** p < 0.001 (t-test).

Figure 7 Effect of ruthenium red on 8-Br-N1-cIDPR mediated Ca²⁺ signalling in intact Jurkat T cells

Jurkat T cells were loaded with Fura-2 and subjected to combined Ca²⁺ imaging and microinjections. Time points of microinjection are indicated by arrows. Cells were microinjected with intracellular buffer (a; n=26), 1 mM 8-Br-N1-cIDPR (b; n=21) or mixture of 10 μM ruthenium red and 1 mM 8-Br-N1-cIDPR (c; n=20). Combined data are shown in (d). Data represent mean ± S.E. of single tracings from time points 50 – 150 s (Ca²⁺ peak). * p < 0.01, ** p < 0.001 (t-test).

Figure 8 Effect of Gd³⁺, SKF and 8-Br-cADPR on Ca²⁺ release and Ca²⁺ entry mediated by 8-Br-N1-cIDPR in intact Jurkat T cells

Jurkat T cells were loaded with Fura-2 and subjected to Ca²⁺ imaging. (a,e,i) Negative control: cells were kept in a nominal Ca²⁺ free buffer in the first part of experiment and buffer was added as indicated. Then, CaCl₂ was readded. (b,f,j) Positive control: 8-Br-N1-cIDPR was added instead of buffer. Cells were preincubated with 10 μM Gd³⁺ (d), 30 μM SKF96365 (h) or 500 μM 8-Br-cADPR (l). Time points of addition of buffer, 1 mM 8-Br-N1-cIDPR or 1 mM Ca²⁺ are indicated by arrows. Characteristic tracings from a representative experiment are shown (a-c, e-g, i-k). Combined data are shown in d,h,l; these data represent mean values ± S.E. (n= 86 to 138) of single tracings from time points 100 to 200 s (8-Br-N1-cIDPR mediated Ca²⁺ release-peak), 300 to 450 s (8-Br-N1-cIDPR mediated Ca²⁺ entry-peak); * p < 0.01, ** p < 0.001 (t-test).

Figure 9 Effect of 8-Br-N1-cIDPR on Ca²⁺ signalling in HEK293 cells overexpressing TRPM2

HEK293 cells transfected with pIRES2-EGFP-TRPM2 (TRPM2, a–c) and pIRES2-EGFP (EGFP/control, d–f) were loaded with Fura-2 and subjected to Ca²⁺ imaging. Time points of addition of a maximal concentration of H₂O₂ (100 or 300 μM; a, d), 1 mM 8-Br-N1-cIDPR (b, e) and buffer (c, f) additions are indicated. Characteristic tracings of a representative experiment are shown (a to f). Concentration-response curve of 8-Br-N1-cIDPR in transfected HEK cells is shown in g (n=6 to 67). Data represent mean ± S.E. of single tracings from time points 100 to 600 s (Ca²⁺ peak).

Figure 10 Activation of endogenous TRPM2 currents in Jurkat T cells by infusion of ADPR, cADPR and 8-Br-N1-cIDPR

All experiments were carried out with 2 mM extracellular Ca²⁺ and with unbuffered intracellular Ca²⁺ similar as described in [35]. Voltage ramps from -85 mV to + 65 mV were applied every 5 s. (a) Representative membrane current over time recorded at -80 mV induced by perfusion with 300 μM ADPR is shown. (b) Representative current-voltage relationship derived from currents evoked by voltage ramps from -85 mV to +65 mV is displayed. (c) Concentration-response relationship for activation of TRPM2 currents by infusion of ADPR (open circle, n=6 to 8), cADPR (open triangle, n=5 to

8) and 300 μM 8-Br-N1-cIDPR (black circle, $n=6$). Data represent mean of maximum current at $-80\text{ mV} \pm \text{S.E.}$ (d) TRPM2 currents at -80 mV after infusion of 30 μM ADPR ($n=8$), co-infusion of 5 μM cADPR/ 30 μM ADPR ($n=9$), 100 μM cADPR/ 30 μM ADPR ($n=8$) and 300 μM 8-Br-N1-cIDPR/ 30 μM ADPR ($n=6$). Data represent mean of maximum current at $-80\text{ mV} \pm \text{S.E.}$ (e) RP-HPLC analysis of cADPR used in the infusion experiments.

Accepted Manuscript

THIS IS NOT THE VERSION OF RECORD - see doi:10.1042/BJ20082308

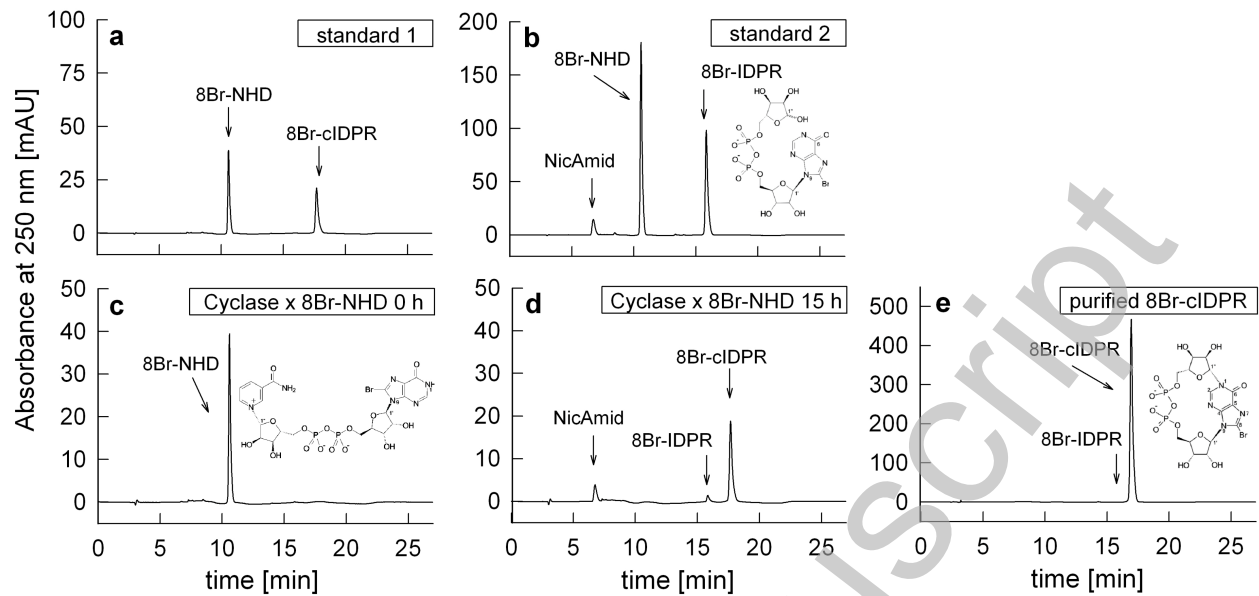
REFERENCES

- 1 De Flora, A., Zocchi, E., Guida, L., Franco, L. and Bruzzone, S. (2004) Autocrine and paracrine calcium signaling by the CD38/NAD⁺/cyclic ADP-ribose system. *Ann. N. Y. Acad. Sci.* **1028**, 176-91
- 2 Guse, A. H. (2004) Biochemistry, biology, and pharmacology of cyclic adenosine diphosphoribose (cADPR). *Curr. Med. Chem.* **11**, 847-55
- 3 Guse, A. H. (2005) Second messenger function and the structure-activity relationship of cyclic adenosine diphosphoribose (cADPR). *FEBS. J.* **272**, 4590-7
- 4 Lee, H. C. (2004) Multiplicity of Ca²⁺ messengers and Ca²⁺ stores: a perspective from cyclic ADP-ribose and NAADP. *Curr. Mol. Med.* **4**, 227-37
- 5 Lee, H. C. (2006) Structure and enzymatic functions of human CD38. *Mol. Med.* **12**, 317-23
- 6 Clapper, D. L., Walseth, T. F., Dargie, P. J. and Lee, H.C. (1987) Pyridine nucleotide metabolites stimulate calcium release from sea urchin egg microsomes desensitized to inositol trisphosphate. *J. Biol. Chem.* **262**, 9561-8
- 7 Lee, H. C., Walseth, T. F., Bratt, G. T., Hayes, R. N. and Clapper, D.L. (1989) Structural determination of a cyclic metabolite of NAD⁺ with intracellular Ca²⁺-mobilizing activity. *J. Biol. Chem.* **264**, 1608-15
- 8 Guse, A. H., Berg, I., da Silva, C. P., Potter, B. V. L and Mayr, G.W. (1997) Ca²⁺ entry induced by cyclic ADP-ribose in intact T-lymphocytes. *J. Biol. Chem.* **272**, 8546-50
- 9 Fruman, D. A., Klee, C. B., Bierer, B. E. and Burakoff, S.J. (1992) Calcineurin phosphatase activity in T lymphocytes is inhibited by FK 506 and cyclosporin A. *Proc. Natl. Acad. Sci. U S A* **89**, 3686-90
- 10 Crabtree, G. R. and Olson, E.N. (2002) NFAT signaling: choreographing the social lives of cells. *Cell* **109 Suppl**, S67-79
- 11 Liu, J., Koyano-Nakagawa, N., Amasaki, Y., Saito-Ohara, F., Ikeuchi, T., Imai, S., Takano, T., Arai, N., Yokota, T. and Arai, K. (1997) Calcineurin-dependent nuclear translocation of a murine transcription factor NFATx: molecular cloning and functional characterization. *Mol. Biol. Cell* **8**, 157-70
- 12 Putney, J. W. J. (1986) A model for receptor-regulated calcium entry. *Cell Calcium* **7**, 1-12
- 13 Putney, J. W. J. (2007) Recent breakthroughs in the molecular mechanism of capacitative calcium entry (with thoughts on how we got here). *Cell Calcium* **42**, 103-10
- 14 Vig, M., Peinelt, C., Beck, A., Koomoa, D. L., Rabah, D., Koblan-Huberson, M., Kraft, S., Turner, H., Fleig, A., Penner, R. and Kinet, J. (2006) CRACM1 is a plasma membrane protein essential for store-operated Ca²⁺ entry. *Science* **312**, 1220-3
- 15 Feske, S., Gwack, Y., Prakriya, M., Srikanth, S., Puppel, S., Tanasa, B., Hogan, P. G., Lewis, R. S., Daly, M. and Rao, A. (2006) A mutation in Orai1 causes immune deficiency by abrogating CRAC channel function. *Nature* **441**, 179-85
- 16 Zhang, S. L., Yu, Y., Roos, J., Kozak, J. A., Deerinck, T. J., Ellisman, M. H., Stauderman, K. A. and Cahalan, M.D. (2005) STIM1 is a Ca²⁺ sensor that activates CRAC channels and migrates from the Ca²⁺ store to the plasma membrane. *Nature* **437**, 902-5
- 17 Guse, A. H., da Silva, C. P., Berg, I., Skapenko, A. L., Weber, K., Heyer, P., Hohenegger, M., Ashamu, G. A., Schulze-Koops, H., Potter, B. V. L and Mayr, G.W. (1999) Regulation of calcium signalling in T lymphocytes by the second messenger cyclic ADP-ribose. *Nature* **398**, 70-3

- 18 Kirchberger, T., Wagner, G., Xu, J., Cordiglieri, C., Wang, P., Gasser, A., Fliegert, R., Bruhn, S., Flügel, A., Lund, F. E., Zhang, L., Potter, B. V. L. and Guse, A.H. (2006) Cellular effects and metabolic stability of N1-cyclic inosine diphosphoribose and its derivatives. *Br. J. Pharmacol.* **149**, 337-344
- 19 Guse, A. H., Roth, E. and Emmrich, F. (1993) Intracellular Ca^{2+} pools in Jurkat T-lymphocytes. *Biochem. J.* **291** (Pt 2), 447-51
- 20 Ben-Nun, A., Wekerle, H. and Cohen, I.R. (1981) The rapid isolation of clonable antigen-specific T lymphocyte lines capable of mediating autoimmune encephalomyelitis. *Eur. J. Immunol.* **11**, 195-9
- 21 Wagner, G. K., Black, S., Guse, A. H. and Potter, B.V.L. (2003) First enzymatic synthesis of an N1-cyclised cADPR (cyclic-ADP ribose) analogue with a hypoxanthine partial structure: discovery of a membrane permeant cADPR agonist. *Chem. Comm.*, 1944-5
- 22 Gasser, A. and Guse, A.H. (2005) Determination of intracellular concentrations of the TRPM2 agonist ADP-ribose by reversed-phase HPLC. *J. Chromatogr. B* **821**, 181-187
- 23 Schweitzer, K., Mayr, G. W. and Guse, A.H. (2001) Assay for ADP-ribosyl cyclase by reverse-phase high-performance liquid chromatography. *Anal. Biochem.* **299**, 218-26
- 24 Kunerth, S., Mayr, G. W., Koch-Nolte, F. and Guse, A.H. (2003) Analysis of subcellular calcium signals in T-lymphocytes. *Cell. Signal.* **15**, 783-92
- 25 Bruzzone, S., Kunerth, S., Zocchi, E., De Flora, A. and Guse, A.H. (2003) Spatio-temporal propagation of Ca^{2+} signals by cyclic ADP-ribose in 3T3 cells stimulated via purinergic P2Y receptors. *J. Cell. Biol.* **163**, 837-45
- 26 Hamill, O. P., Marty, A., Neher, E., Sakmann, B. and Sigworth, F.J. (1981) Improved patch-clamp techniques for high-resolution current recording from cells and cell-free membrane patches. *Pflugers Arch. Eur. J. Physiol.* **391**, 85-100
- 27 Fliegert, R., Gasser, A. and Guse, A.H. (2007) Regulation of calcium signalling by adenine-based second messengers. *Biochem. Soc. Trans.* **35**, 109-14
- 28 Kolisek, M., Beck, A., Fleig, A. and Penner, R. (2005) Cyclic ADP-ribose and hydrogen peroxide synergize with ADP-ribose in the activation of TRPM2 channels. *Mol. Cell* **18**, 61-9
- 29 Togashi, K., Hara, Y., Tominaga, T., Higashi, T., Konishi, Y., Mori, Y. and Tominaga, M. (2006) TRPM2 activation by cyclic ADP-ribose at body temperature is involved in insulin secretion. *EMBO. J.* **25**, 1804-15
- 30 Langhorst, M. F., Schwarzmann, N. and Guse, A.H. (2004) Ca^{2+} release via ryanodine receptors and Ca^{2+} entry: major mechanisms in NAADP-mediated Ca^{2+} signaling in T-lymphocytes. *Cell. Signal.* **16**, 1283-9
- 31 Kerschbaum, H. H. and Cahalan, M.D. (1999) Single-channel recording of a store-operated Ca^{2+} channel in Jurkat T lymphocytes. *Science* **283**, 836-9
- 32 Herscher, C. J. and Rega, A.F. (1996) Pre-steady-state kinetic study of the mechanism of inhibition of the plasma membrane $\text{Ca}(2+)\text{-ATPase}$ by lanthanum. *Biochemistry* **35**, 14917-22
- 33 Zhang, B., Wagner, G. K., Weber, K., Garnham, C., Morgan, A. J., Galione, A., Guse, A. H. and Potter, B.V.L. (2008) 2'-deoxy cyclic adenosine 5'-diphosphate ribose derivatives: importance of the 2'-hydroxyl motif for the antagonistic activity of 8-substituted cADPR derivatives. *J. Med. Chem.* **51**, 1623-36

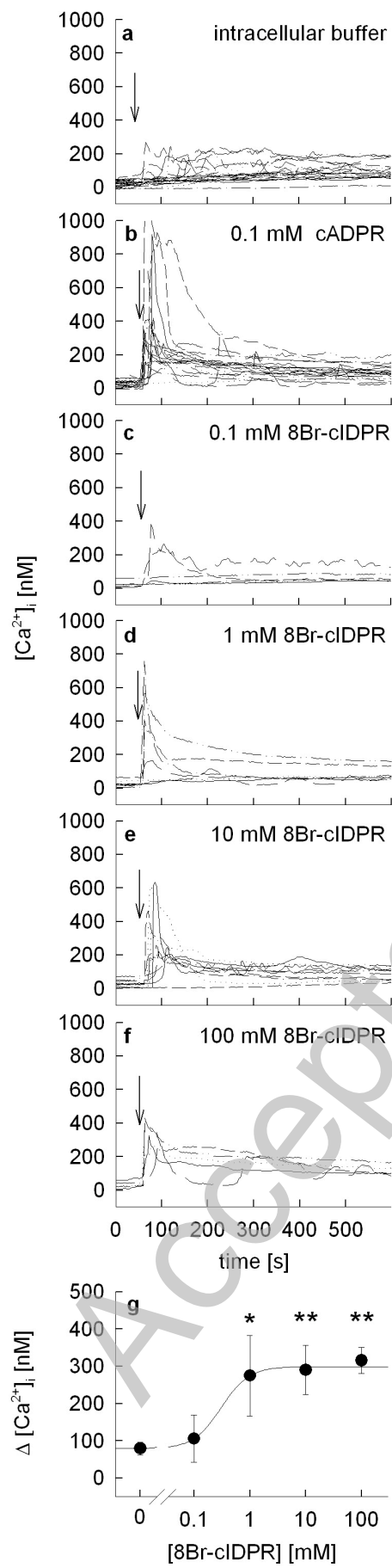
- 34 Kiselyov, K., Shin, D. M., Shcheynikov, N., Kurosaki, T. and Muallem, S. (2001) Regulation of Ca^{2+} -release-activated Ca^{2+} current (Icrac) by ryanodine receptors in inositol 1,4,5-trisphosphate-receptor-deficient DT40 cells. *Biochem. J.* **360**, 17-22
- 35 Beck, A., Kolisek, M., Bagley, L. A., Fleig, A. and Penner, R. (2006) Nicotinic acid adenine dinucleotide phosphate and cyclic ADP-ribose regulate TRPM2 channels in T lymphocytes. *FASEB. J.* **20**, 962-4
- 36 Gasser, A., Bruhn, S. and Guse, A.H. (2006) Second messenger function of nicotinic acid adenine dinucleotide phosphate revealed by an improved enzymatic cycling assay. *J. Biol. Chem.* **281**, 16906-13
- 37 Guse, A. H. and Lee, H.C. (2008) NAADP: A Universal Ca^{2+} Trigger. *Sci. Signal.* **1**, re10
- 38 Guse, A. H., Goldwisch, A., Weber, K. and Mayr, G.W. (1995) Non-radioactive, isomer-specific inositol phosphate mass determinations: high-performance liquid chromatography-micro-metal-dye detection strongly improves speed and sensitivity of analyses from cells and micro-enzyme assays. *J. Chromatogr. B Biomed. Appl.* **672**, 189-98
- 39 Gu, X., Yang, Z., Zhang, L., Kunerth, S., Fliegert, R., Weber, K., Guse, A. H. and Zhang, L. (2004) Synthesis and biological evaluation of novel membrane-permeant cyclic ADP-ribose mimics: N1-[(5"-O-phosphorylethoxy)methyl]-5'-O-phosphorylinosine 5',5"-cyclicpyrophosphate (cIDPRE) and 8-substituted derivatives. *J. Med. Chem.* **47**, 5674-82
- 40 Guse, A. H., Gu, X., Zhang, L., Weber, K., Kramer, E., Yang, Z., Jin, H., Li, Q., Carrier, L. and Zhang, L. (2005) A minimal structural analogue of cyclic ADP-ribose: synthesis and calcium release activity in mammalian cells. *J. Biol. Chem.* **280**, 15952-9
- 41 Kudoh, T., Fukuoka, M., Ichikawa, S., Murayama, T., Ogawa, Y., Hashii, M., Higashida, H., Kunerth, S., Weber, K., Guse, A. H., Potter, B. V. L., Matsuda, A. and Shuto, S. (2005) Synthesis of stable and cell-type selective analogues of cyclic ADP-ribose, a Ca^{2+} -mobilizing second messenger. Structure-activity relationship of the N1-ribose moiety. *J. Am. Chem. Soc.* **127**, 8846-55
- 42 Moreau, C., Wagner, G. K., Weber, K., Guse, A. H. and Potter, B.V.L. (2006) Structural determinants for N1/N7 cyclization of nicotinamide hypoxanthine 5'-dinucleotide (NHD^+) derivatives by ADP-ribosyl cyclase from *Aplysia californica*: Ca^{2+} -mobilizing activity of 8-substituted cyclic inosine 5'-diphosphoribose analogues in T-lymphocytes. *J. Med. Chem.* **49**, 5162-76
- 43 Xu, J., Yang, Z., Dammermann, W., Zhang, L., Guse, A. H. and Zhang, L. (2006) Synthesis and agonist activity of cyclic ADP-ribose analogues with substitution of the northern ribose by ether or alkane chains. *J. Med. Chem.* **49**, 5501-12
- 44 Schwarzmann, N., Kunerth, S., Weber, K., Mayr, G. W. and Guse, A.H. (2002) Knock-down of the type 3 ryanodine receptor impairs sustained Ca^{2+} signaling via the T cell receptor/CD3 complex. *J. Biol. Chem.* **277**, 50636-42
- 45 Parekh, A. B., Fleig, A. and Penner, R. (1997) The store-operated calcium current I(CRAC): nonlinear activation by InsP_3 and dissociation from calcium release. *Cell* **89**, 973-80

Fig1



Accepted Manuscript

Fig2



THIS IS NOT THE VERSION OF RECORD - see doi:10.1042/BJ20082308

Fig 3

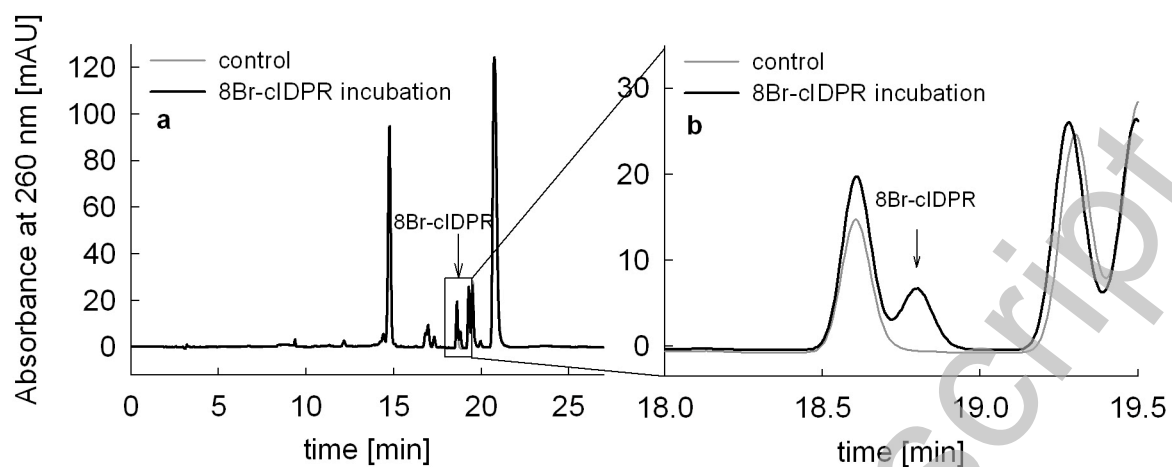
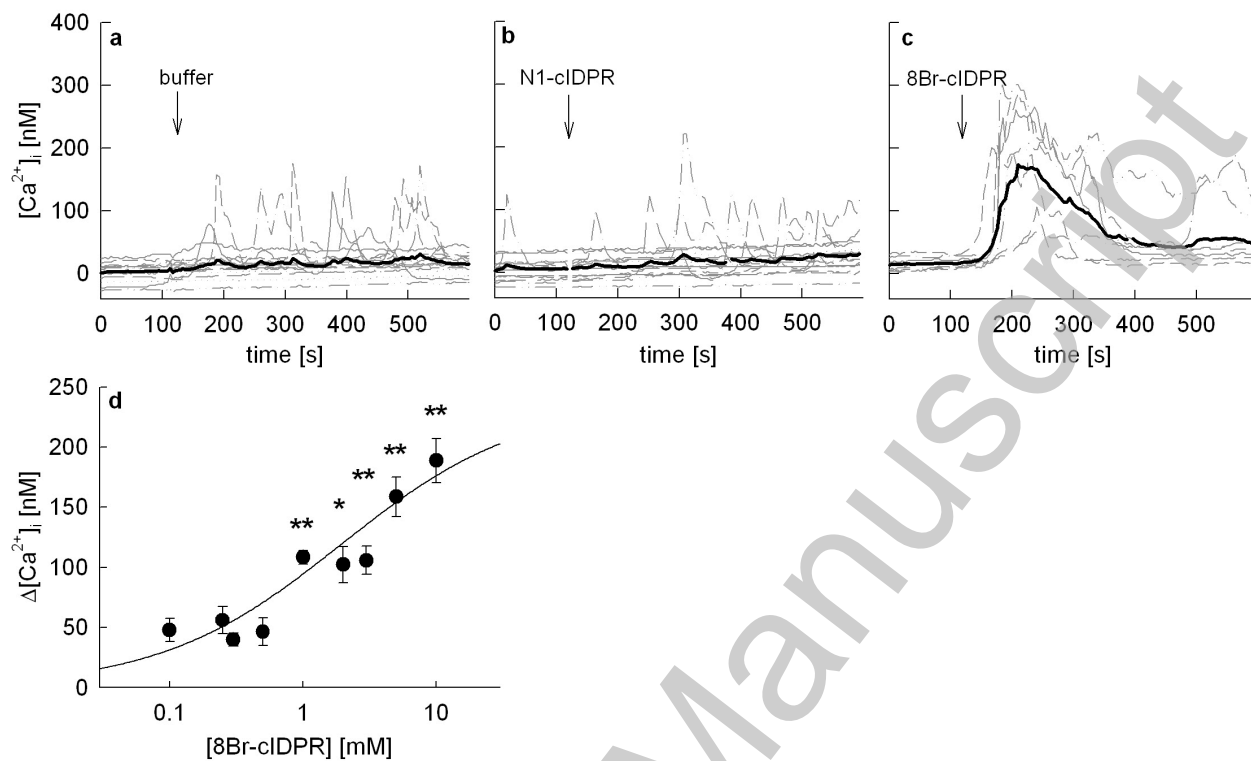


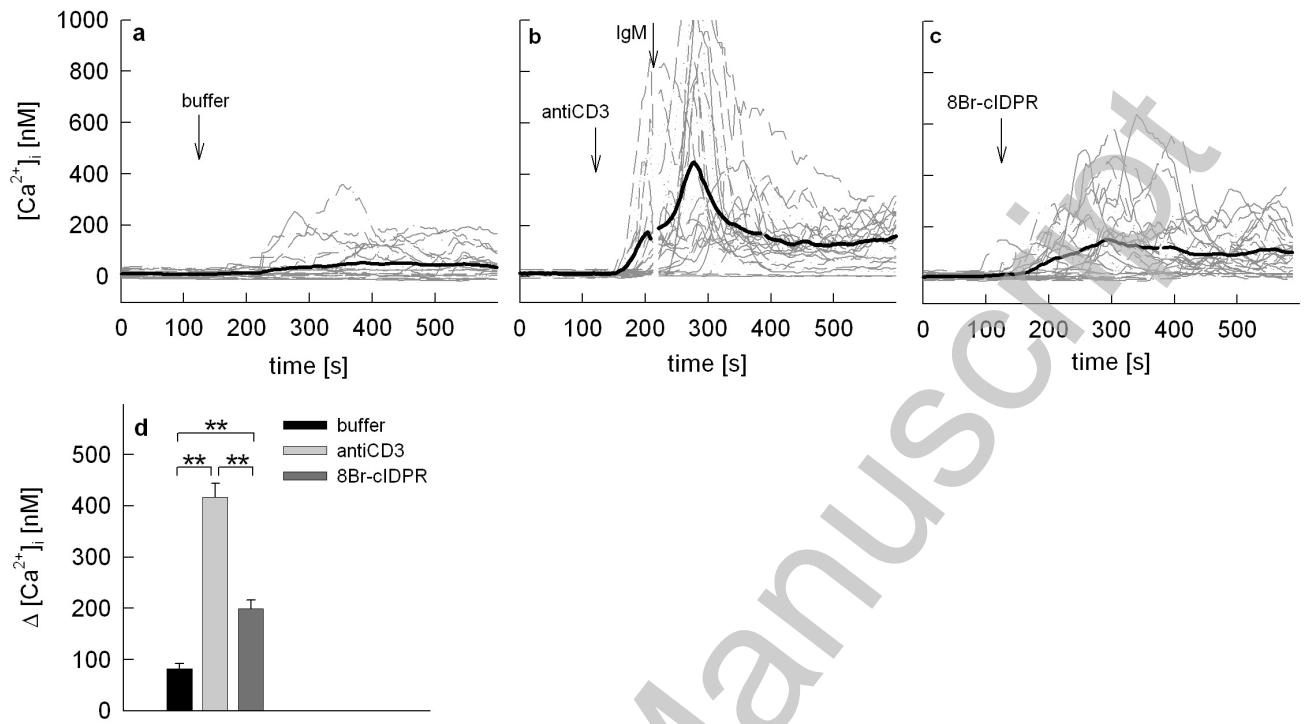
Fig 4



THIS IS NOT THE VERSION OF RECORD - see doi:10.1042/BJ20082308

Accepted Manuscript

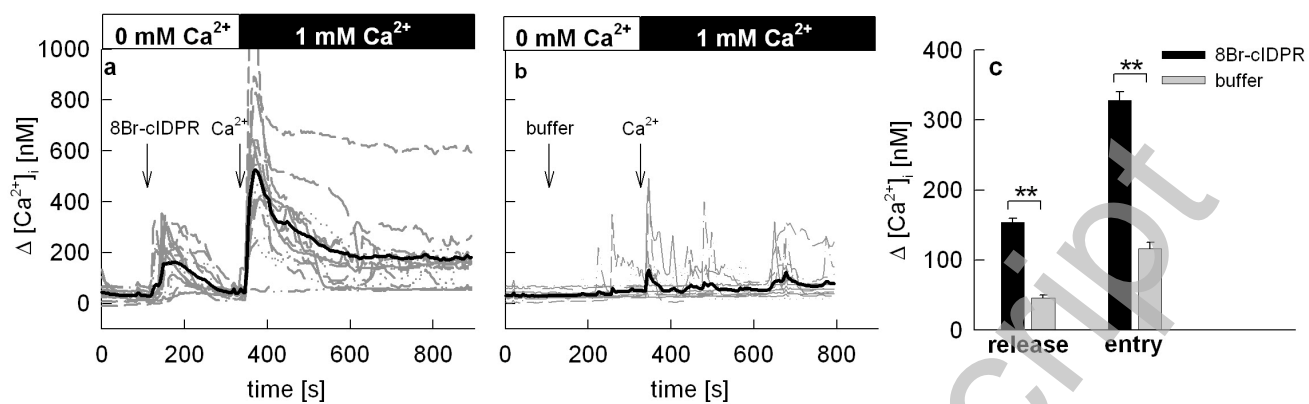
Fig 5



THIS IS NOT THE VERSION OF RECORD - see doi:10.1042/BJ20082308

Accepted Manuscript

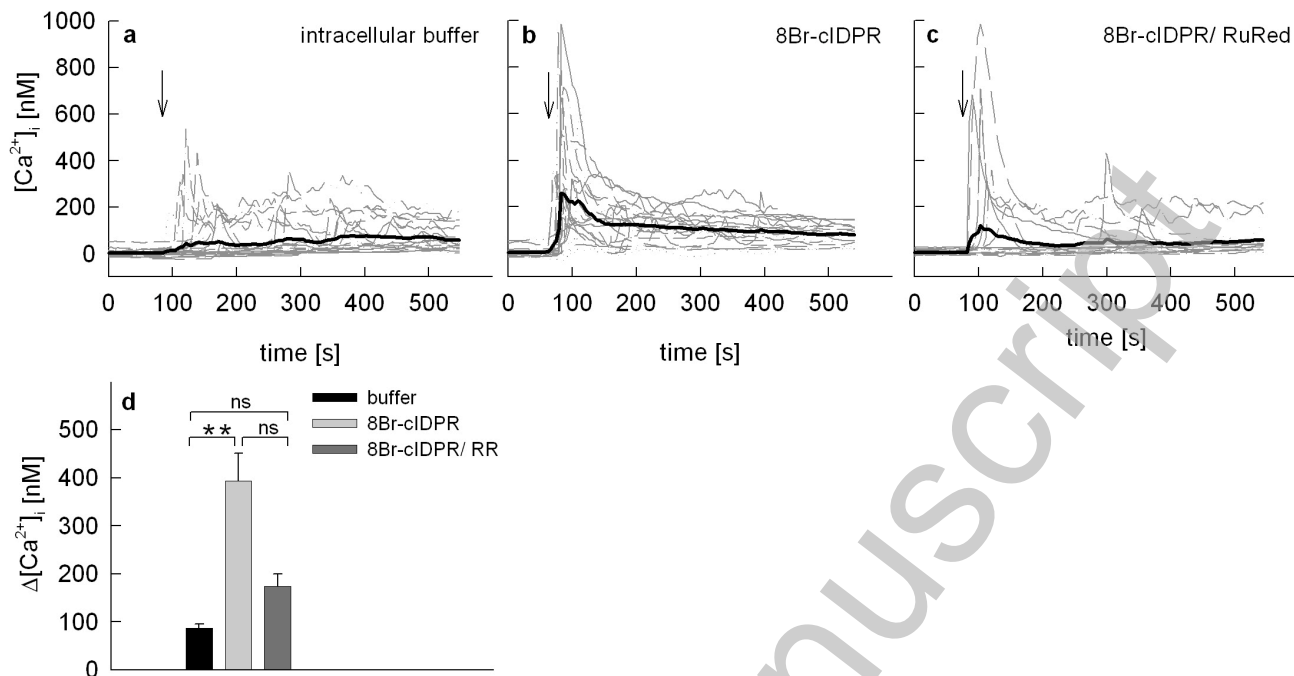
Fig6



THIS IS NOT THE VERSION OF RECORD - see doi:10.1042/BJ20082308

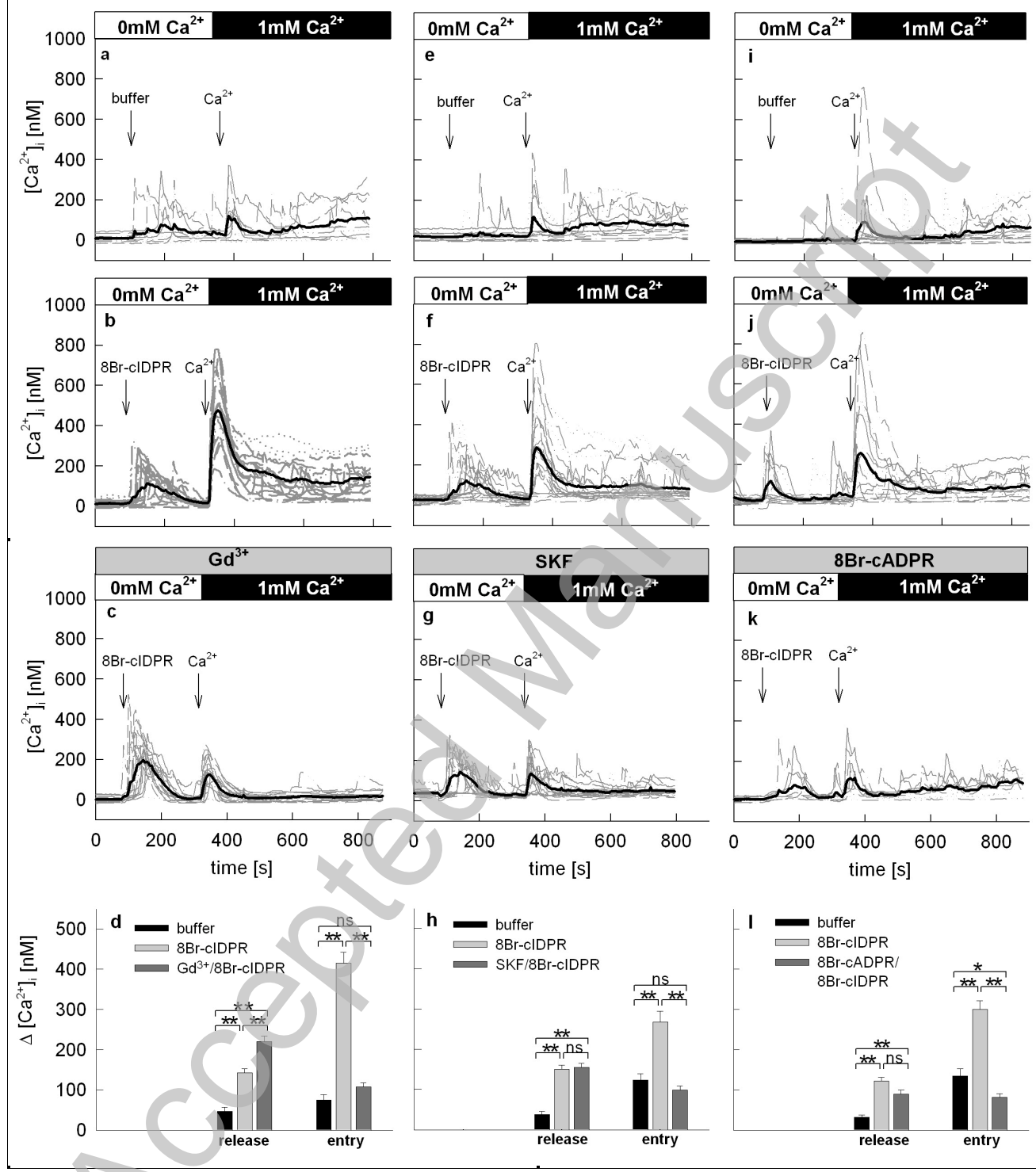
Accepted Manuscript

Fig7



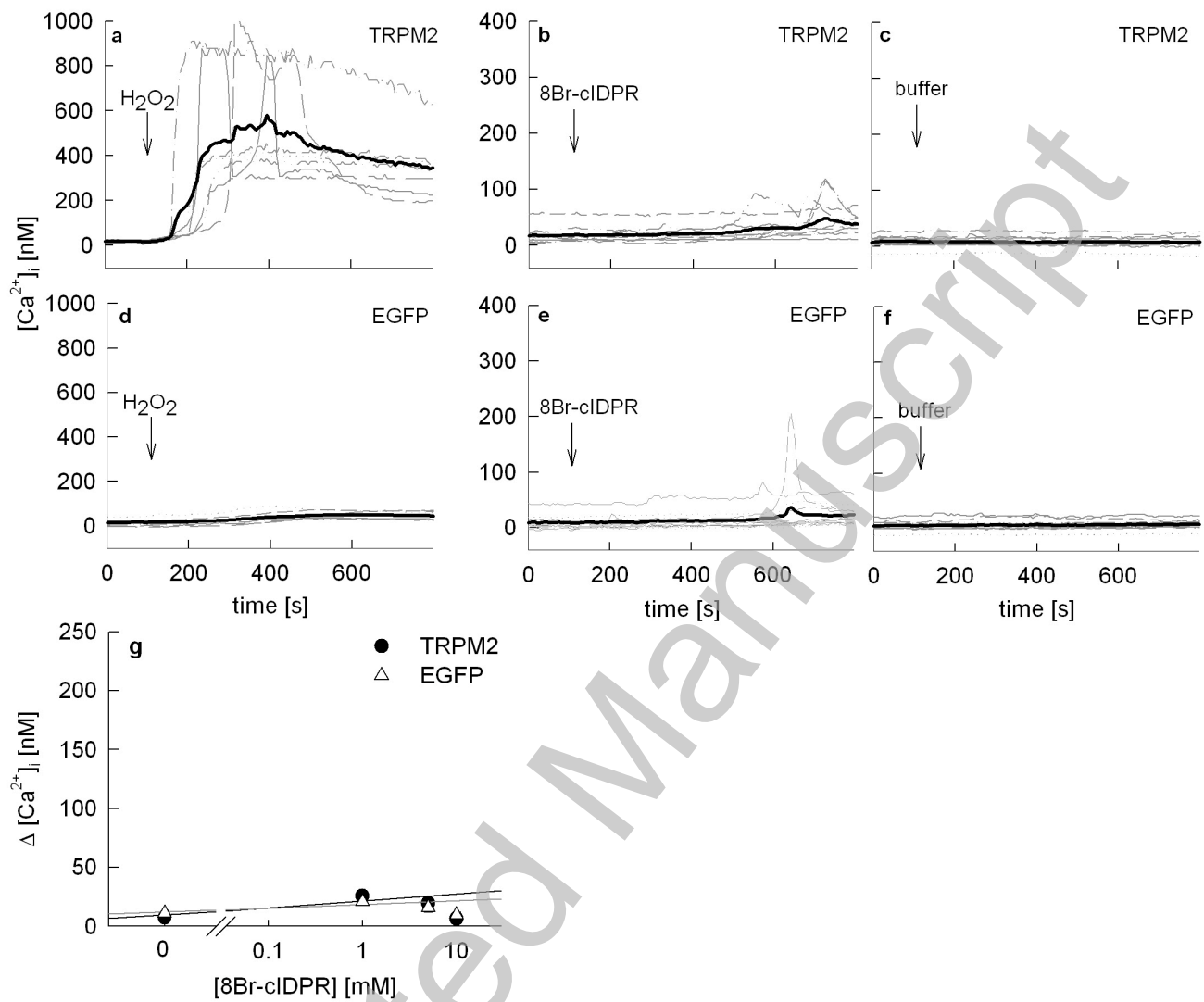
Accepted Manuscript

Fig8



THIS IS NOT THE VERSION OF RECORD - see doi:10.1042/BJ20082308

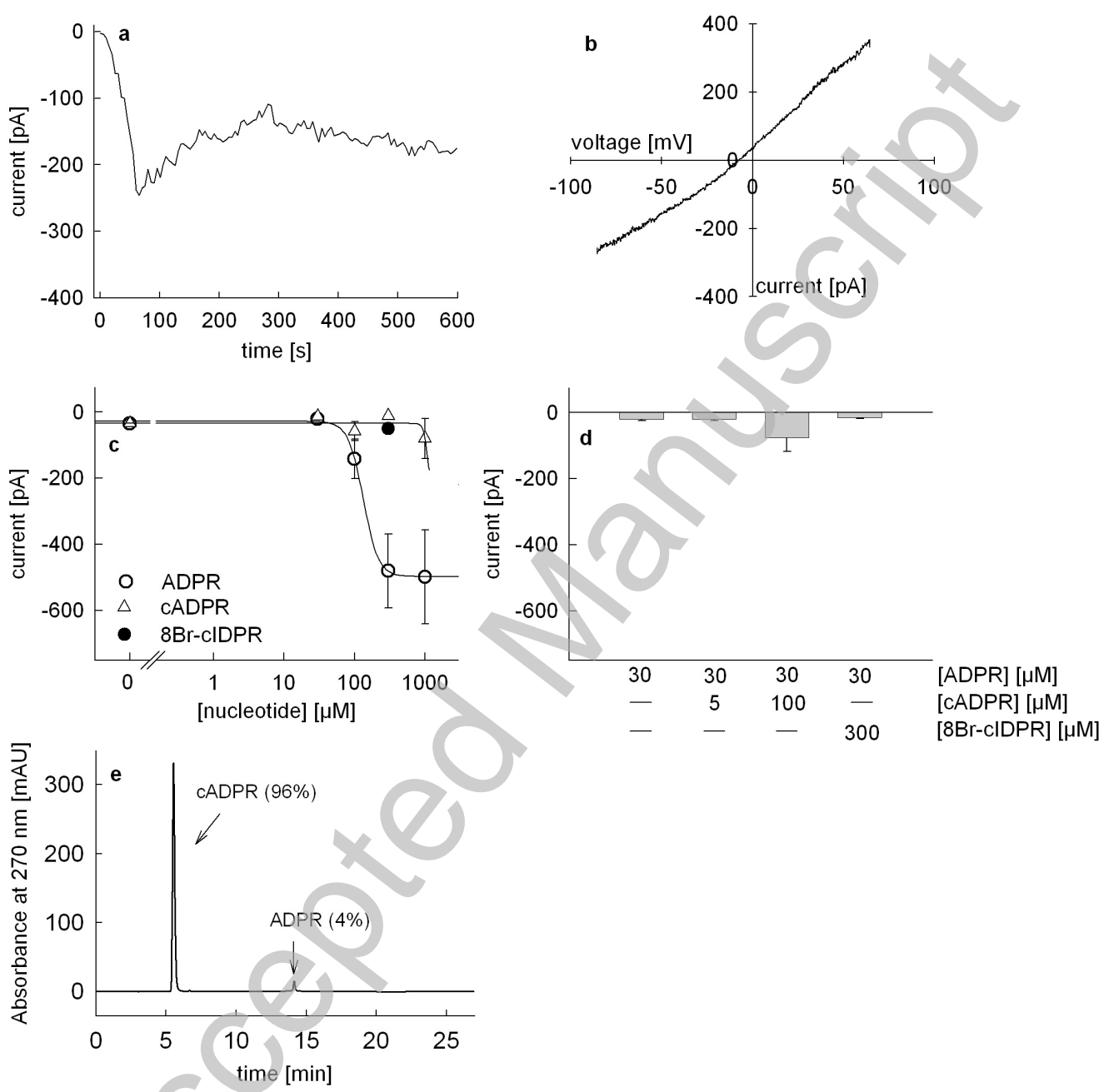
Fig9



THIS IS NOT THE VERSION OF RECORD - see doi:10.1042/BJ20082308

Accepted Manuscript

Fig10



THIS IS NOT THE VERSION OF RECORD - see doi:10.1042/BJ20082308

Accepted Manuscript